JOURNAL OF MATERIALS SCIENCE 20 (1985) 4593–4600

Electrical conductivity of yttria-stabilized zirconia single crystals

SOTOMITSU IKEDA, OSAMU SAKURAI, KEIZO UEMATSU, NOBUYASU MIZUTANI, MASANORI KATO
Department of Inorganic Materials, Faculty of Engineering, Tokyo Institute of Technology, Ookayama, Meguro-ku, Tokyo 152, Japan

The electrical conductivities of YSZ single crystals with various compositions covering FSZ and PSZ regions were measured by a complex impedance method and a four-probe a.c. method. The conductivities changed significantly as a function of composition. A simple conduction model for PSZ showed that the tetragonal phase is a good oxygen ionic conductor having an activation energy for motion of about 0.8 to 0.9 eV. It is promising for low temperature application of a solid state electrolyte.

1. Introduction

Partially stabilized zirconia (PSZ), as well as fully stabilized zirconia (FSZ), is becoming increasingly important as a solid state electrolyte because of its good electrical and mechanical properties [1]. However, most of the present knowledge of these materials is based on the results from polycrystalline specimens. Complicated microstructures, especially grain boundaries and cubic tetragonal interfaces in PSZ, are expected to affect the electrical properties. Careful study on single crystalline specimens is needed to understand further the electrical properties of PSZ and FSZ.

Difficulties associated with the microstructure are believed to be overcome, at least in principle, by a.c. electrical measurements and complex admittance representation [2–4]. They were widely used for separating several contributions on the total impedance of specimens [4–7]. However, the ideal semicircle in the representation on which the method is based is rarely observed in real ceramic specimens [8]. A clear explanation of this incomplete semicircle is not given. Direct measurement on well characterized single crystals can also eliminate many difficulties associated with microstructures.

The specimens used in the present work are yttria-stabilized zirconia (YSZ) made by the Xe-arc image floating zone method in our laboratory. The characteristics of the specimens are presented separately (to be published). Specimens with 2 to 4 mol % $YO_{1.5}$ are mostly the monoclinic phase but also contain a small amount of tetragonal and/or cubic phase. They contain microcracks resulting from the monoclinic–tetragonal transformation. The specimens with 5 to 14 mol % $YO_{1.5}$ are opaque and consist of tetragonal and cubic phases. In particular, the specimens with 5 to 10 mol % $YO_{1.5}$ have small lens-shaped precipitates of the tetragonal phase in the cubic matrix phase as shown in Fig. 1.

Quite recently, since energy dispersive X-ray spectroscopy (EDS) enabled us to obtain microchemical information from micrometre sized areas it became clear that the cubic matrix phase has about 11 mol % $YO_{1.5}$ and that the tetragonal precipitates have about 3 mol % $YO_{1.5}$ in every PSZ specimen annealed at 1700° C. It suggests that all two-phase structures are in equilibrium. These PSZ specimens contain interfaces between the cubic and tetragonal phases, but no grain boundary. The specimens with more than 16 mol % $YO_{1.5}$ are transparent and have only a cubic phase. They clearly contain neither interface nor grain boundary.

In the present work we measured the electrical conductivity of the single crystalline PSZ and FSZ by a complex impedance method and also by a four-probe a.c. method. The relationship

0022–2461/85 $03.00 + .12

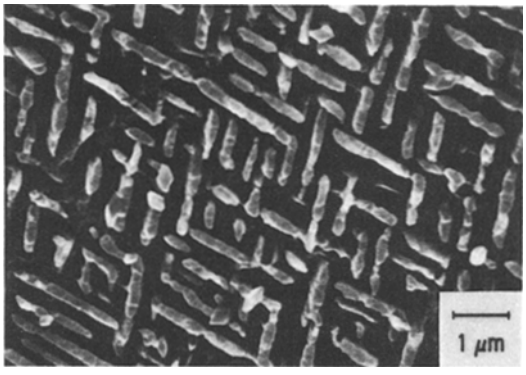

Figure 1 Scanning electron micrograph of the 9 mol % $YO_{1.5}$–ZrO_2 single crystal polished and etched by phosphoric acid.

between electrical conductivity and the phase present is discussed. The conductivity of the tetragonal phase was determined using a simple conduction model for PSZ containing cubic and tetragonal phases, and its characteristics are discussed in detail.

2. Experimental procedure

The specimens were crystals grown by the Xe-arc image floating zone method in air. Zirconium oxide and yttrium oxide (both reagent grade) were used as starting materials. Details of the growth procedure and characterization of the crystals are presented elsewhere [9]. Crystals were annealed at 1700° C for 24 h in air before cutting to obtain specimens with similar thermal history.

A complex impedance method and a four-probe a.c. method were applied for the electrical conductivity measurements. The samples for the complex impedance method were thin slices of crystal cut perpendicular to the growth direction (3 mm diameter × 0.5 mm). Silver paste electrodes were applied to both faces and fired at 600° C. The impedances were measured between 250 and 600° C in air with a Vector Impedance Meter (HP model 4800A) at 5 Hz to 550 kHz. The samples used for the four-probe a.c. method were crystals of cylindrical cut (3 mm diameter × 7 to 10 mm). Fine platinum electrodes were attached to the specimens with platinum paste. The conductivity was measured with an LCR meter (YHP model 4261A, C‖R, 1 kHz) at 350 to 1000° C, in air with a heating rate of approximately 5° C min^{-1}, and a cooling rate of 6° C min^{-1}. Runs were repeated on several specimens to confirm the reproducibility.

3. Results

3.1. Complex impedance method

With this method in the high temperature region, the complex impedance of a single crystalline specimen at a given temperature was constant without any significant shift over the entire frequency region (5 Hz to 550 kHz). The impedance was purely resistive, and represents the bulk resistance of the specimens. A measurement made at any single frequency gives accurate bulk resistivity. At low temperature, however, the bulk resistivity increases, and the capacitive component becomes increasingly important with decreasing temperature in complex impedance. A full Cole–Cole plot was required to resolve the bulk resistivity of the specimen.

Fig. 2 shows representative Cole–Cole plots of specimens having various structures at low temperatures. Curve (a) shows the result for PSZ with 6 mol % $YO_{1.5}$. This specimen has precipitations of tetragonal phase in the cubic matrix as shown in Fig. 1. Curve (b) shows the result for FSZ with 16 mol % $YO_{1.5}$. This specimen is fully stabilized and contains only cubic phase. Curve (c) shows the result for a polycrystalline specimen with 16 mol % $YO_{1.5}$. This specimen is compositionally the same as that of Curve (b), but contains grain boundaries and pores.

In single crystalline samples, only one arc was found in the complex impedance plane under all conditions. This made interpretation very simple. The impedance determined from the intersect of the semicircle and abscissa is attributed to the lattice conductivity. Analysis of the curve of the single crystalline PSZ sample shows that this has d.c. conductivity of $3.28 \times 10^{-6} \Omega^{-1} cm^{-1}$ and a relative permittivity of 118 at 275° C. Boundaries between the tetragonal and cubic phases apparently have no significant effect on Cole–Cole plots. Single crystalline FSZ has a d.c. conductivity of $1.58 \times 10^{-6} \Omega^{-1} cm^{-1}$ and a relative permittivity of 81 at 280° C. These values were similar to those for single crystalline PSZ. In polycrystalline FSZ samples, two arcs were found. They arose from the lattice and grain boundary conductivities [3]. Their d.c. conductivities are 1.43×10^{-5} and

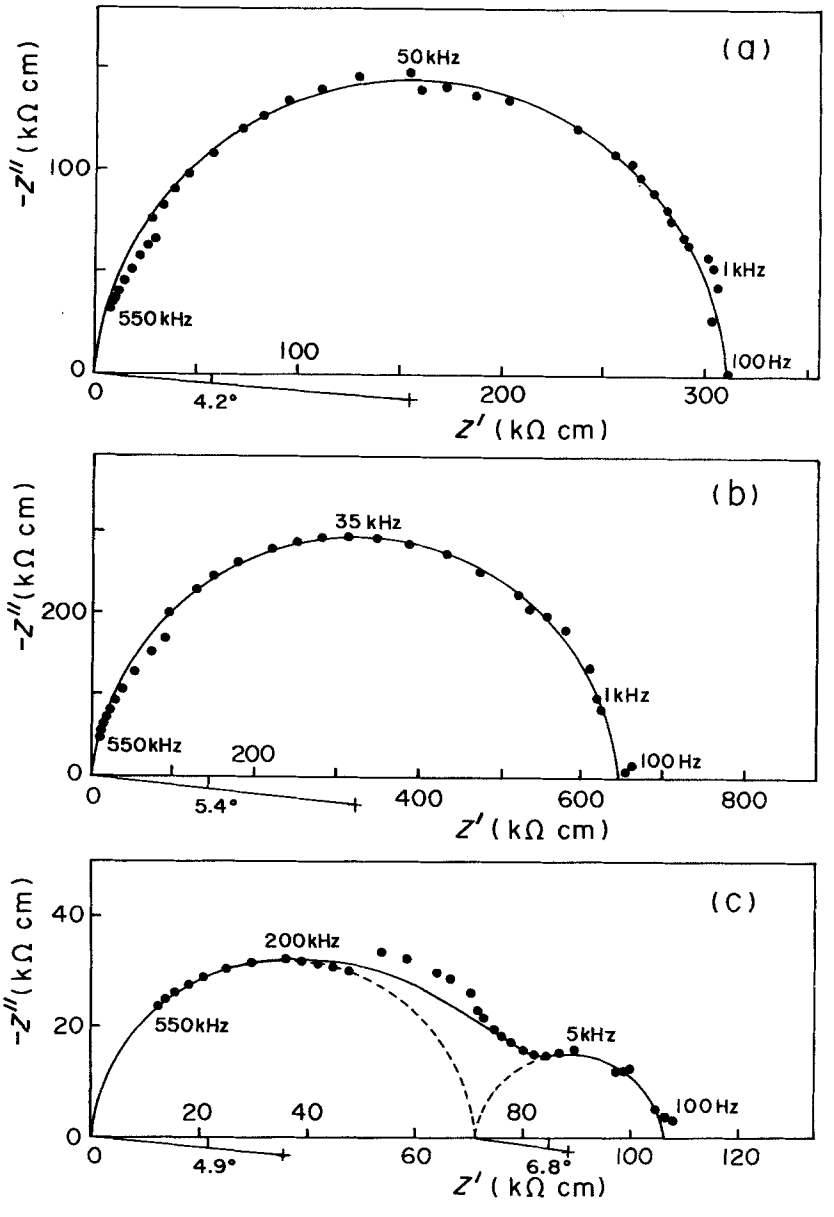

Figure 2 Complex impedance plots obtained at about 300° C for YSZ samples: (a) 6 mol % $YO_{1.5}$–ZrO_2 single crystal (PSZ) at 275° C; (b) 16 mol % $YO_{1.5}$–ZrO_2 single crystal (FSZ) at 280° C; (c) 16 mol % $YO_{1.5}$–ZrO_2 polycrystal (FSZ) at 340° C.

$2.88 \times 10^{-5} \Omega^{-1} cm^{-1}$, and their relative permittivities are 129 and 10 400 at 340° C, respectively.

The d.c. conductivities measured by the complex impedance method were plotted for the reciprocal of an absolute temperature in Fig. 3. The Arrhenius plot showed a straight line for 250 to 600° C.

3.2. Four-probe a.c. method

The temperature dependences of conductivities measured by the four-probe a.c. method are shown in Fig. 4.

With this method, the results fundamentally agreed with those obtained by the complex impedance method. However, an anomaly of conductivity appeared in specimens having 5 to 9 mol % $YO_{1.5}$, showing a slightly high conductivity in the low temperature region. The Arrhenius plot deviates from the straight line in this region. The source of this anomaly was probably due to instrumental limitation. With the equipment applied for measurement, the conductivity was estimated from a single measurement made at one frequency, 1 kHz. An

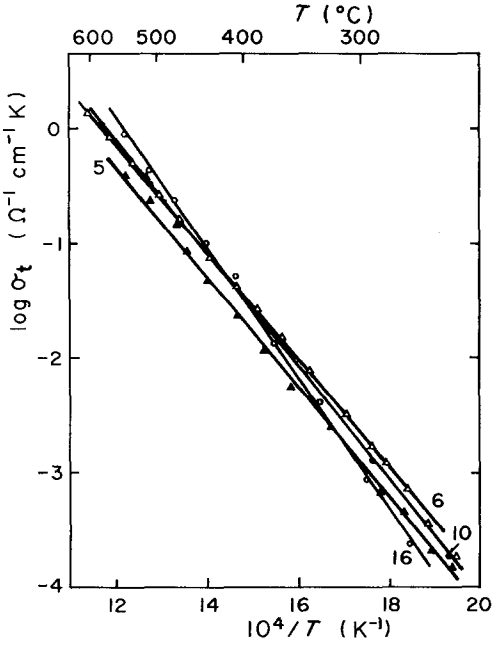

Figure 3 Arrhenius plots of conductivity determined by the complex impedance method for various YSZ single crystals: the number indicates mol % $YO_{1.5}$.

ideal parallel connection of pure resistance and capacitance was assumed instrumentally in the LCR meter in complex impedance representation. This is apparently inadequate for the low conductivity region where significant deviation from the ideal was found in the semicircle. For this region, we tentatively adopt the results obtained by the complex impedance method.

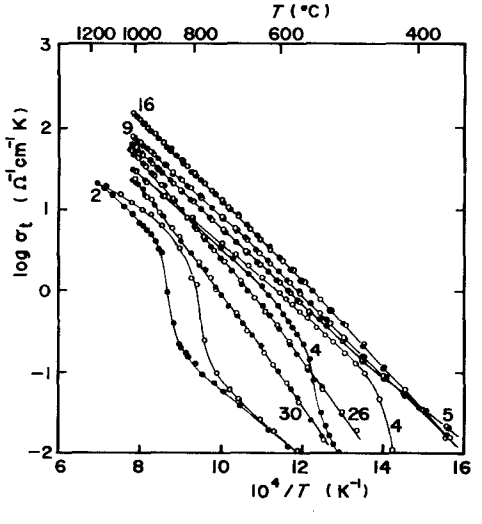

Figure 4 Arrhenius plots of conductivity determined by the four-probe a.c. method for various YSZ single crystals: the number indicates mol % $YO_{1.5}$ (●: heating, ○: cooling).

2 and 4 mol % $YO_{1.5}$–ZrO_2 specimens which had many microcracks, show hysteresis in the Arrhenius plots during the heating and cooling cycles. The conductivities during the heating and cooling cycles followed different paths for each cycle. This hysteresis can be related to the monoclinic–tetragonal phase transformation in the specimens [6, 10, 11]. DTA measurements on these samples shows an endothermic peak and an exothermic peak in the temperature region corresponding to the hysteresis during the heating and cooling runs, respectively.

5 to 9 mol % $YO_{1.5}$–ZrO_2 specimens show two deflection points in the Arrhenius plots. In the case of 9 mol % $YO_{1.5}$–ZrO_2 specimens, a deflection point at about 500° C during the heating run was due to the anomaly explained above. A subsequent high temperature deflection point at about 700° C shows bulk property. Examples of activation energies calculated from the slopes of Arrhenius plots for 9 mol % $YO_{1.5}$–ZrO_2 are 0.89 eV above 690° C, and 1.05 eV at 480 to 690° C.

10 to 30 mol % $YO_{1.5}$–ZrO_2 specimens show only one deflection point in the Arrhenius plots as in previous studies [6, 8, 12–14]. The activation energies of 16 mol % $YO_{1.5}$–ZrO_2 were 0.97 eV above 540° C and 1.09 eV below 540° C. Good agreement was found between the result obtained by complex impedance and a four-probe a.c. methods.

Figs. 5, 6 and 7 show, respectively, the changes with yttria content of the conductivity σ, activation energy, E, and pre-exponential term A of the general equation

$$\sigma = A/T \exp(-E/kT) \qquad (1)$$

Electrical conductivities change significantly with composition. At high temperature above 800° C, they increased with yttria content up to 8 mol % $YO_{1.5}$, did not change markedly at 8 to 12 mol % $YO_{1.5}$, increased again up to 16 mol % $YO_{1.5}$, and decreased at higher $YO_{1.5}$ content. This tendency is similar to those of other studies [6, 13–21]. Conductivity shows small maxima in the region of PSZ at low temperature. This behaviour has not been reported in the past. The $YO_{1.5}$ content giving the maximum electrical conductivity tended to decrease with decreasing temperature. The maximum of conductivity shifted to 14 mol % $YO_{1.5}$ at 400° C.

Results shown in Fig. 6 were calculated by a

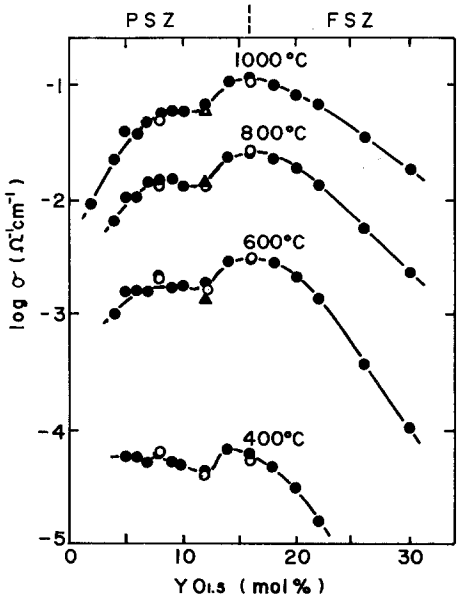

Figure 5 Isothermal conductivities as a function of composition in YSZ.

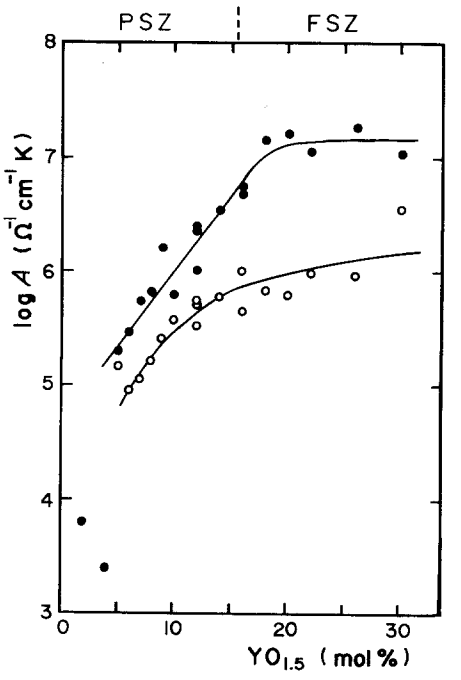

Figure 7 Pre-exponential term A of Equation 1 as a function of composition in YSZ: ●, low temperature region determined by four-probe a.c. method; ○, high temperature region determined by four-probe a.c. method.

method of least squares for the intervals of low and high temperature regions separated by the deflection point. In general, the activation energy increased with increasing $YO_{1.5}$ content, and was low in PSZ. This is the first report which clearly shows the low activation energy of PSZ. This result agreed with previous expectations [21, 22]. In the cubic phase region, the increase of activation energy by increasing $YO_{1.5}$ content accords with past studies [6, 13–18].

Fig. 7 shows the dependence of the pre-exponential term A on composition. It increased with increasing $YO_{1.5}$ content. The slope in this increase is steeper in the region of PSZ than in FSZ, where it is nearly constant. From Fig. 9 it is clear that the high conductivity of PSZ at low temperature is mainly due to low activation energy for carrier motion.

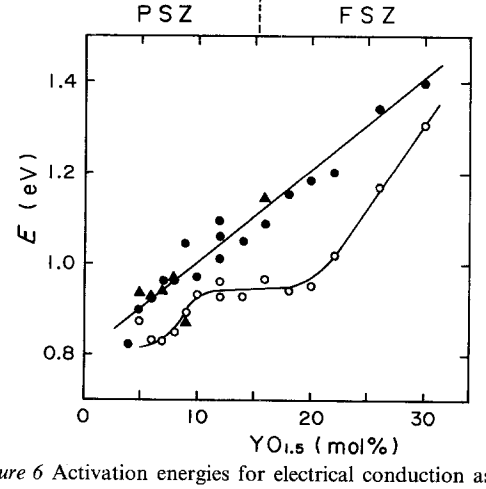

Figure 6 Activation energies for electrical conduction as a function of composition in YSZ: ○, high temperature region determined by four-probe a.c. method; ●, low temperature region determined by four-probe a.c. method; ▲, low temperature region determined by complex impedance method.

4. Discussion

The absence of complicated microstructure made the measurement and analysis very simple and straightforward. High conductivity of PSZ in the low temperature region is clarified without ambiguity in this study, supporting the high ionic conduction of the tetragonal phase reported by Gupta *et al.* [22] and Bonanos *et al.* [23] in polycrystalline tetragonal YSZ. The results on FSZ basically agreed to those in previous polycrystalline studies [13–21]. In the following, we focus our discussion mainly on the electrical property of PSZ and the tetragonal phase.

Semiquantitative analysis is presented to isolate the electrical property of the tetragonal phase. Two extreme cases were considered in this analysis. The equivalent circuits for the electrical response of the PSZ single crystal are shown in Fig. 8. One is the complex

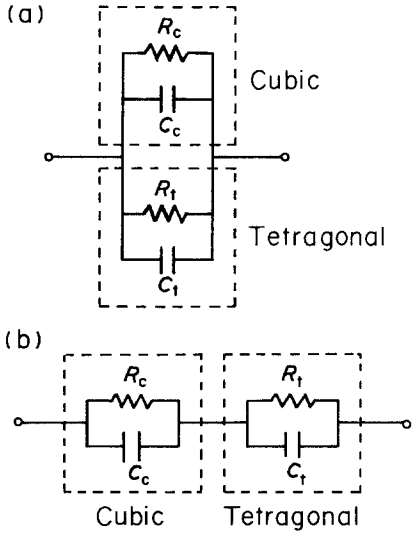

Figure 8 Equivalent circuits for the electrical response of PSZ containing cubic and tetragonal phases (a) in parallel and (b) in series.

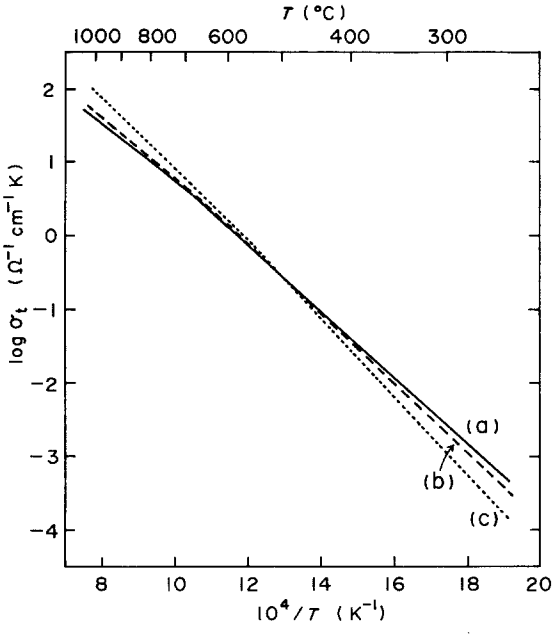

Figure 9 Arrhenius plots of calculated conductivity for the tetragonal phase in 6 mol % $YO_{1.5}$–ZrO_2 single crystal, (a) using parallel and series models. (b), (c) The experimental data for 6 and 12 mol % $YO_{1.5}$–ZrO_2 single crystals, respectively.

conductivities of the cubic and tetragonal phases in parallel (a), and the other in series (b). In both cases the complex conductivity σ^* is defined by

$$\sigma^* = \sigma + j\omega\varepsilon \quad (2)$$

where σ is the conductivity, ε the absolute permittivity, ω the angular frequency of the alternating electric field and j an imaginary unit. The complex conductivity equation of PSZ single crystal derived from Figs. 8a and b are, respectively

$$\sigma^* = (1 - x_t)\sigma_c^* + x_t\sigma_t^* \quad \text{for (a)} \quad (3)$$

$$\frac{1}{\sigma^*} = \frac{1 - x_t}{\sigma_c^*} + \frac{x_t}{\sigma_t^*} \quad \text{for (b)} \quad (4)$$

where σ^*, σ_c^* and σ_t^* are the complex conductivities of the PSZ specimen, cubic and tetragonal phase, respectively. The volume fraction of tetragonal phase x_t was determined by a point counting method on the scanning electron micrograph of the specimen surfaces polished and etched by phosphoric acid. The details of the procedure are presented separately [24]. The σ_c was assumed to be equal to the conductivity of 12 mol % $YO_{1.5}$–ZrO_2 because the composition of the cubic matrix in PSZ annealed at 1700° C was found to be about 11 mol % $YO_{1.5}$ owing to the results of energy dispersive X-ray spectroscopy.

Application of a series equivalent circuit to the present case may look unreasonable at first sight. Two semicircles might be expected for this model. However, substitution of the appropriate parameters shows that only one semicircle virtually appears in the complex impedance representation. This was due to the very similar electrical properties of the cubic and tetragonal phases.

The conductivities of the tetragonal phase calculated from Equations 3 and 4 almost agreed, and are shown in Fig. 9 with the original data measured by the complex impedance and four-probe a.c. methods. No difference in conductivities of the tetragonal phase calculated by the series model and a parallel model suggests that the conductivity of the tetragonal phase is nearly equal to that of the cubic phase. Fig. 9 suggests that the Arrhenius plot of the tetragonal phase can be divided into two regions. At low temperature the calculated conductivities of the tetragonal phase are higher than the original data of PSZ and the cubic phase in PSZ, while at high temperature the calculated conductivities are lower than the original data. The activation energies for electrical conduction of the tetragonal phase derived from 6 mol % $YO_{1.5}$–ZrO_2 were 0.78 eV at above 700° C and 0.88 eV below 700° C. These values approximately agree with those reported by Gupta *et al.* [22]. They reported

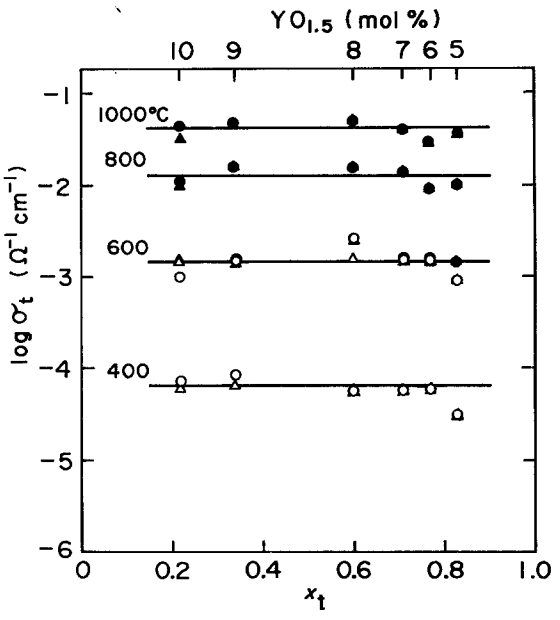

Figure 10 Isothermal conductivities of the tetragonal phase as a function of their volume fraction in PSZ: ● and ▲, series and parallel model determined by four-probe a.c. method; ○ and △, series and parallel model determined by complex impedance method.

that the activation energies of tetragonal zirconia with 1.4 mol % Y_2O_3 were 0.91 to 0.94 eV at 300 to 600° C and decreased above 600° C.

The electrical conductivites of the tetragonal phase in PSZ are shown as a function of the volume fraction x_t in Fig. 10, and σ_t appears to be constant in PSZ. This result agreed with our expectations, because the composition of the tetragonal phase in PSZ annealed at 1700° C is constant in all two-phase structures in equilibrium, and the conductivity should be constant. It was also found that σ_t was high, especially at low temperature. The activation energies of the tetragonal phase in PSZ are also constant for the volume fraction x_t, about 0.73 to 0.85 eV at high temperature and 0.87 to 0.95 eV at low temperature. These values of the tetragonal phase are significantly lower than those of the cubic phase.

The concentration of electrical carriers in PSZ is expectedly low. Phase diagrams for YSZ [25–27] show that our PSZ specimens annnealed at 1700° C consist of the cubic phase having about 11 mol % $YO_{1.5}$, and the tetragonal phase having about 3 mol % $YO_{1.5}$. The tetragonal phase in PSZ contains approximately 1.5 mol % oxygen vacancies, while the cubic phase with 16 mol % $YO_{1.5}$, which shows a maximum in electrical conductivities as a function of composition, contains 8 mol % oxygen vacancies. The concentration of oxygen vacancies in the tetragonal phase is only one-fifth of that in FSZ. In general, the electrical conductivity is proportional to the concentration of the electrical carrier and its mobility, which is a function of the activation energy; the lower the activation energy is, the larger the mobility is. High conductivity of the tetragonal phase in the present study results from its low activation energy for motion. Low activation energy in PSZ becomes increasingly effective for higher conductivity at low temperature. This shows that PSZ is clearly a very promising oxygen ionic conductor especially for low temperature application.

References

1. M. IWASE, *Kotaibutsuri* **16** (1981) 217.
2. H. IWAHARA, *Kagaku* **38** (1983) 397.
3. J. E. BAUERLE, *J. Phys. Chem. Solids* **30** (1969) 2657.
4. H. S. ISAACS and L. J. OLMER, *J. Electrochem. Soc.* **129** (1982) 436.
5. M. J. VERKERK, B. J. MIDDELHUIS and A. J. BURGGRAAF, *Solid State Ionics* **6** (1982) 159.
6. R. E. W. CASSELTON, *Phys. Status Solidi (a)* **2** (1970) 571.
7. M. MIYAYAMA, H. INOUE and H. YANAGIDA, *Commun. Amer. Ceram. Soc.* **66** (1983) 164.
8. P. ABELARD and J. F. BAUMARD, *Phys. Rev. B* **26-2** (1982) 1005.
9. S. SAKURAI, Y. YOKOTANI, K. ŪEMATSU, N. MIZUTANI and M. KATO, *Nippon Kagaku Kaishi (J. Chem. Soc. Jpn.)* **9** (1981) 1396.
10. P. KOFSTAD and D. J. RUZICKA, *J. Electrochem. Soc.* **110** (1963) 181.
11. R. W. VEST and T. M. TALLAN, *J. Amer. Ceram. Soc.* **48** (1965) 472.
12. S. P. S. BADWAL, *J. Mater. Sci.* **19** (1984) 1767.
13. T. TAKAHASHI, *Ouyou-butsuri* **49** (1980) 956.
14. D. K. HOHNKE, in "Fast Ion Transport in Solids", edited by P. Vashishta, J. N. Mundy and G. K. Shen (Elsevier, North Holland, 1979) p. 669.
15. J. E. BAUERLE and J. HRIZO, *J. Phys. Chem. Solids* **30** (1969) 565.
16. J. M. DIXON, L. D. LaGRANGE, U. MERTEN, C. F. MILLER and J. T. PORTER, II, *J. Electrochem. Soc.* **110** (1963) 276.
17. F. A. KROGER, *J. Amer. Ceram. Soc.* **49** (1966) 215.
18. H. SCHMALZRIED, *Z. Phys. Chem.* **105** (1977) S.47.
19. D. W. STRICKLER and W. G. CARLSON, *J. Amer. Ceram. Soc.* **48** (1965) 286.
20. R. E. CARTER and W. L. ROTH, GE Research Center Report 67-C (1968) p. 308.
21. M. MORINAGA, J. B. COHEN and J. FABER Jr, *Acta Crystallogr.* **A35** (1979) 789.

22. T. K. GUPTA, R. B. GREKILA and E. C. SUBBARAO, *J. Electrochem. Soc.* **128** (1981) 929.
23. N. BONANOS, R. K. SLOTWINSKI, B. C. H. STEELE and E. P. BUTLER, *J. Mater. Sci. Lett.* **3** (1984) 245.
24. N. MIZUTANI and M. KATO, unpublished results.
25. H. G. SCOTT, *J. Mater. Sci.* **10** (1975) 1527.
26. V. S. STUBICAN, R. C. HINK and S. P. RAY, *J. Amer. Ceram. Soc.* **61** (1978) 17.
27. C. PASCUAL and P. DURAN, *ibid.* **66** (1983) 23.

Received 14 January
and accepted 31 January 1985